ANNALS of Faculty Engineering Hunedoara – International Journal of Engineering
Tome XX [2022] | Fascicule 1 [February]

[1.]Nilanjan MUKHOPADHYAY, [2.]Saswati DEY, [3.]Jyotipriya SEN, [4.]Swati DAS, [5.]Kunal DAS

STUDY ON DIFFERENT ASPECTS OF BUILDING EXTRACTION PROCESS BASED ON MORPHOLOGICAL BUILDING INDEX FROM REMOTELY SENSED IMAGES

[1-5.]Department of Electronics & Communication Engineering, Global Institute of Management and Technology, Krishnagar, Nadia 741102, INDIA

Abstract: An emerging field of research in the area of remote sensing is the automatic building extraction from High-Resolution remotely sensed images. Of late various researchers have followed different methods for building extraction such as edge detection, geometric and also based on object-based methods. A very recent method or approach for automatic building extraction or indication in remotely sensed images is the Morphological building index (MBI) that can detect buildings of different sizes and shapes. However, an image captured from zenith position of the satellite will have a different appearance from that of the non-zenith position in terms of object reflectance. In this study different aspects of morphological image processing for building extraction based on the position of the image capturing platform have been discussed. This morphological image processing relies on White Top-hat transformation followed by erosion operation to extract buildings. The extracted buildings can further be processed for rooftop solar panel installation purposes.

Keywords: building extraction; morphological image processing; remote sensing; top-hat transformation; satellite image processing

1. INTRODUCTION

Now a days, the field of automatic building extractions from remotely sensed high resolution images has a deep inter connection with different sectors specifically Automatic creation of 3D urban city maps. The geometric data obtained from the maps could be linked with various applications, among them natural disaster management i.e., flooding, earthquakes, defence monitoring, urban planning and airport hazard analysis belong to the major category. However, these application areas are increasing by leaps and bounds as many new sectors are being connected with it such as identification of rooftop areas for solar panel installation. Improvisation of Remote sensing and GIS techniques have added extra milage to the Automatic creation of 3D urban city maps. In the field of remote sensing, the contribution of high-resolution earth satellites, such as, IKONOS and QUICKBIRD for identifications of different features, like road, building, tree present on the earth's surface play a major role. Performance of all these applications relied on effective and accurate extraction of information or data from remotely sensed imagery. Human operated semi-automated systems, where manual extraction of buildings by drawing lines and curves that indicates buildings walls and borders have dominated over the years. Often, these processes are time consuming and expensive with a low update rate which have paved the way for automation in building extraction with very less human interference. Hurdles faced by automatic building extraction process includes various structure and shape of buildings along with the presence of obstacles due to surrounding objects that may lowered the contrast between roof of building and surrounding region. Of late various filters have been proposed to extract edges based on different detection techniques. The main pillar on which majority of previous works in the sector of building detection are standing is that the detection model has a quadrilateral shape as the image footprints are quadrilateral [1-5]. They have followed edge/line detection techniques such as, Canny, DoG, Laplace, etc which can successfully detect large buildings with flat rooftops but have poor performance in in cluttered scene scenarios or scenes including small buildings. The footprint detection and 3D reconstruction have been described with the application of lines, regions, planar patches, polyhedral shapes, geometrical models, and multiple images [6-9]. Among the other approaches a segmentation method introduced by Cheng et al [10] where 2D histograms have been used for segmenting the aerial images into four distinctive regions. A modified partial snake model was reported for detection of buildings. A sophisticated surface fitting method has been reported with the implementation of image corners [12-13]. A method based on edge detection to detect flat roofs buildings using geometric and projective constraints has been proposed by Lin and Nevatia [14]. However, this detection method has success over rectangular buildings only. A comparative study on building extraction techniques from aerial images has been done by Mayer, highlighting the advantages and limitations of different techniques [1]. For extraction of large buildings, a supervised clustering and edge detection-based technique applied on panchromatic images taken from QUICKBIRD has been proposed [15], but it is not suitable for small buildings having little or no shadow. Jin & Davis followed a relatively complicated procedure using IKONOS satellite imagery to extract small buildings [16]. Huang and Zhang [17] introduced Morphological Building Index (MBI) in an object-based framework to increase the accuracy of building extraction techniques. Moreover, Singh and Mehrotra have introduced Differential Morphological shadow and building operator to extract buildings from Geoeye-1 imagery of the city Washington DC Mall [18].

Various semi-automated systems have illustrated different difficulties associated with faithful extraction of buildings such as, variation in shape, size and texture of building rooftops in urban area. However, there are benefits as well as serious limitations of these techniques and it is needless to mention that a highly reliable system for robust detection and identification of buildings is yet to appear. A limited number of systems have analysed the effects of Morphological image processing on the images taken from different positions of the satellite or drone. There will be certain difference between the images taken from zenith position of satellite or drone with that of the non-zenith position in terms of reflectance from the objects present in the image. An attempt to find out the orientation angle of a building cluster in dense urban areas have been done by Sohn and Dowman using IKONOS imagery based on Fourier analysis [19]. However, faithful extraction has not been achieved as a small number of overall features is used for building identification. In this present communication, a comprehensive study on the effects of applying Morphology-based techniques using images taken from both the zenith and non-zenith position of the satellite or drone has been put forward. Since, mathematical Morphology-based techniques are gaining importance because of the fact that both gradient- and Laplacian-based filters are very sensitive to noise, Top-hat transformation along with Morphological Building Index (MBI) and Differential morphological profile (DMP) have been used in this present study.

The rest of the study is organized as follows. Section II describes the methodology for building extraction that has guided the present research followed by the simulation results and discussions on the effects of capturing platform position in Section III. Section IV illustrates the conclusion that is followed by reference.

2. THEORY & METHODOLOGY

An automatic building extraction technique following morphological image processing is based on simultaneous retrieval of three information i.e., firstly, structural information is extracted from morphological profiles, then contextual information for buildings followed by spectral information for final detection. The concept for developing MBI is to create a connection of the implicit characteristics of buildings based on brightness, size, and contrast with the morphological operators (e.g., top-hat by reconstruction etc.) used as proposed by Huang and Zhang [17]. At last, buildings are extracted by putting a threshold on the MBI feature image. This technique is more effective for automatic building extraction from high-resolution imagery. In this current section, the mathematical model of MBI and the steps for automatic building extraction have been elaborated. Figure 1 illustrates the steps for automatic building extraction based on MBI. In the process of developing MBI the knowledge about implicit characteristics of buildings i.e., brightness, size, and contrast as well as their importance in building extraction are very essential. Brightness of the pixel corresponds to the maximum value of a pixel at all the visible bands that have major spectral information of buildings. The brightness value for pixel x is recorded as its [20]:

$$b(x) = \max_{1 \le k \le k}(\mathrm{band}_{k(x)}) \tag{1}$$

where, band_k(x) represents the spectral value of pixel *x* at the *kth* spectral band and the number of multispectral bands is denoted by *k*.

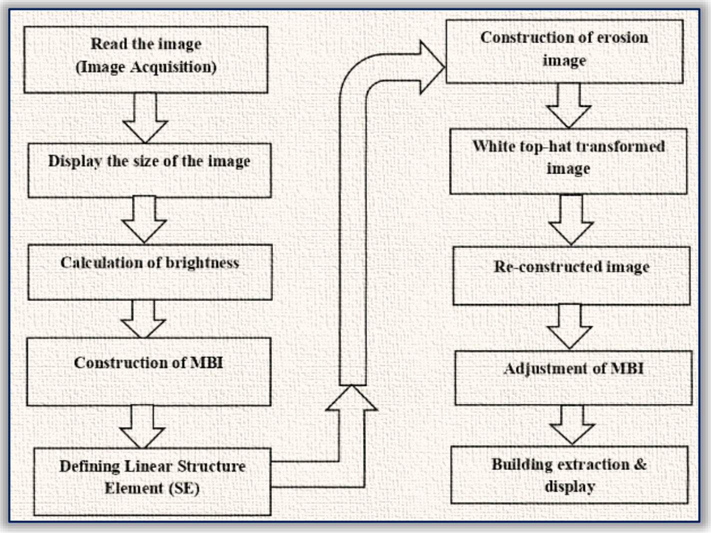

Figure 1. Methodology followed for automatic building extraction

The contrast between high reflective rooftops and the shadows adjacent to the buildings are represented by the differential morphological profiles (DMP) of the white top-hat. The formation of linear structural elements (SE) is next crucial task for construction of a building index as it has to filter out roads on the basis of size and directionality that have very similar spectral reflectance as buildings. The length-width ratio is taken into account for removal of narrow and elongated structures. After defining the SE, having proper size and direction re-construction of the image is obtained through erosion function. This process will help to find image that Differential morphological profiles (DMP) is obtained by white top-hat transformation based on re-constructed image.

The mathematical representation of White top-hat by reconstruction (W-TH) is given by:

$$\mathrm{W-TH(d,s)} = \mathrm{b} - \mathrm{y_b^{re}(d,s)} \tag{2}$$

Where, length and direction of a linear SE are indicated by s and d respectively and the opening-by-reconstruction of the brightness image is indicated by $\mathrm{y_b^{re}}$ [20].

Morphological profiles (MP) of the white top-hat are obtained by following the relations,

$$\mathrm{MP_{w-TH}(d,s)} = \mathrm{W-TH(d,s)}$$
$$\mathrm{MP_{w-TH}(d,0)} = \mathrm{b} \tag{3}$$

The Differential morphological profiles (DMP) of the white top-hat are given as,

$$\mathrm{DMP_{w-TH}(d,s)} = \left|\mathrm{MP_{w-TH}}(\mathrm{d},(\mathrm{s}+\Delta\mathrm{s})) - \mathrm{MP_{w-TH}(d,s)}\right| \tag{4}$$

where length of the linear SE belongs to $\mathrm{s_{min}} \leq \mathrm{s} \leq \mathrm{s_{max}}$ with an interval between the profiles denoted as $\Delta\mathrm{s}$. The morphological building index (MBI) which is the average of DMP of the white top-hat can be obtained from the following relation, i.e.,

$$\mathrm{MBI} = \frac{\sum_{\mathrm{d,s}} \mathrm{DMP_{w-TH}(d,s)}}{\mathrm{D \times S}} \tag{5}$$

where the numbers of directionality and scale of the profiles are indicated by D and S respectively. In this study the value of D is chosen as 4 i.e., considering four directions. However, accuracy for building detection does not depend on higher value of D.

Depending on the spatial characteristics of buildings and the spatial resolution, sizes of SE i.e., $\mathrm{s_{max}}$, $\mathrm{s_{min}}$ and $\Delta\mathrm{s}$ have been decided. The number of scales can be obtained by using the formula,

$$\mathrm{S} = \frac{(\mathrm{s_{max}} - \mathrm{s_{min}})}{\Delta\mathrm{s}} + 1 \tag{6}$$

In the final detection of buildings larger MBI values are preferred for structures in most of the directions as since they show high local contrast in these directions.

3. SIMULATION RESULTS & DISCUSSION

In the present section two images from two different position of the capturing platform have been considered. First, a satellite-based image taken from the zenith position and next a drone- based image captured from non-zenith position. Both the images refer to different geographical location on earth. The simulation is performed on MATLAB 2009a in a laptop with 2 GB RAM, Dual Core processor and Windows10 operating system. The effects of position of capturing platform as well as the variation of length of linear structural elements (SE) on the final output image have been analysed.

— Drone based image of NABANNA building area Kolkata, India

A drone-based image of NABANNA building situated at Kolkata, India has been considered for the first case study. The image as shown in Figure. 2 has three visible bands along with 720X721 pixels. The image includes buildings with variable reflectance and structure, low intensity vegetation, roads, etc. Clearly the image is captured from non-zenith position resulting in reflectance difference between the near side buildings with that of the far side. The range of pixels intensity lies within 2 to 255 referring low to bright extremum. As mentioned earlier that the sizes of SE i.e., $\mathrm{s_{max}}$, $\mathrm{s_{min}}$ and $\Delta\mathrm{s}$ depends on the spatial resolution so for first condition respective values are chosen as $\mathrm{s_{max}} = 50$, $\mathrm{s_{min}} = 2$ and $\Delta\mathrm{s} = 2$.

Figure 2. Drone based image of NABANNA building area, Kolkata, India

The number of scales can be obtained by using equation 6 and it is S=25. In the process of obtaining white top-hat transformation by reconstruction, multiple erosion of the input image is performed using element in SE in succession. Figure. 3 represents 8 nos. of erosion images (total 25 erosion images) that have been obtained using morphological opening operation to preserve the shape and size of larger objects in the image while eroding the image.

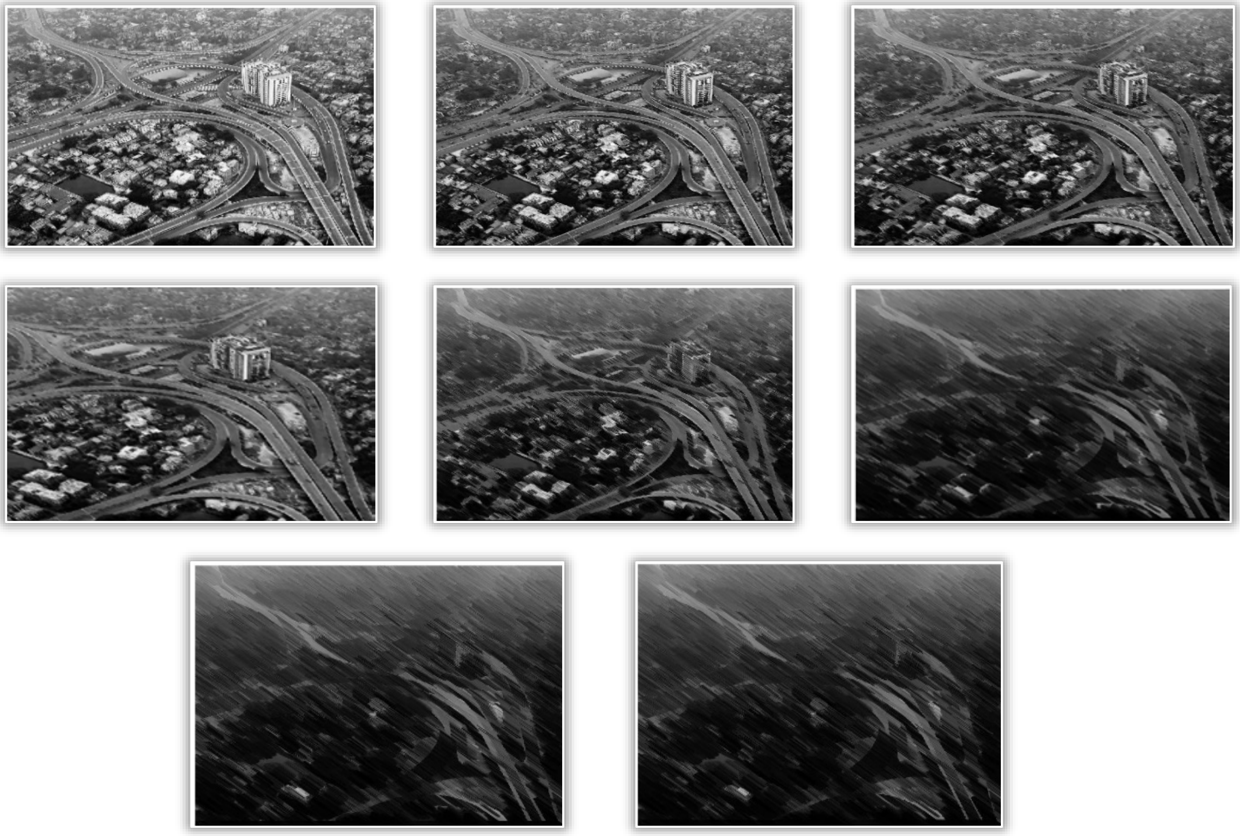

Figure 3. Eroded images obtained using morphological opening operation

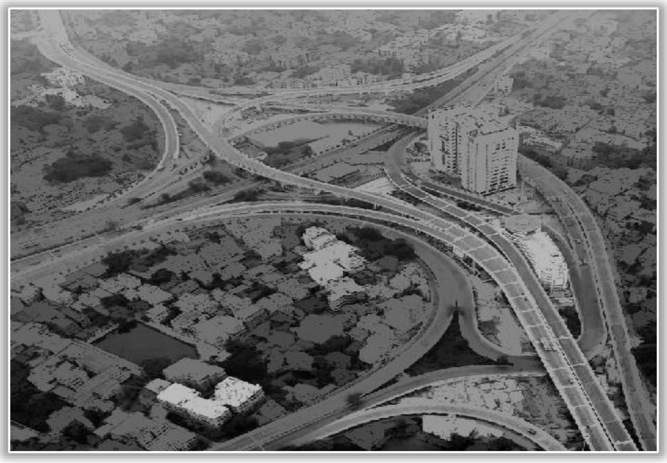

Figure 4. Morphologically reconstructed image

Morphological reconstruction is performed using those erosion images as marker, based on the characteristics of another image, called the mask. The process begins from peaks, in the marker image and continues until the image values stop changing. In the morphologically reconstructed output image, all the intensity fluctuations except the intensity peak have been removed. Figure. 4 illustrates the morphologically reconstructed image.

Over the length of linear SE i.e., $s_{min} \leq s \leq s_{max}$, differential morphological profiles (DMP) of the white top-hat are obtained with Δs interval between the profiles. The DMPs are important in highlighting contrast between high reflective rooftops and the shadows adjacent to the buildings. In Figure 5 all the 25 nos. of DPM (*S*=25), that have been obtained from measuring variation of morphological profile values for each element in SE are illustrated.

Considering the values of directionality and scale of the profiles (*D*=4 and *S*=25 in this case) MBI can be calculated. Depending on obtained MBI value filtering of buildings can be performed by adjusting intensity value in the final image. Using *imadjust* function the thresholding operation is performed that maps the intensity values in final grayscale image in such a way that 1% of data is saturated at low and high intensities of operated image to increase the contrast of the output image. In Figure 6 the final output image indicating extracted buildings is shown along with input image.

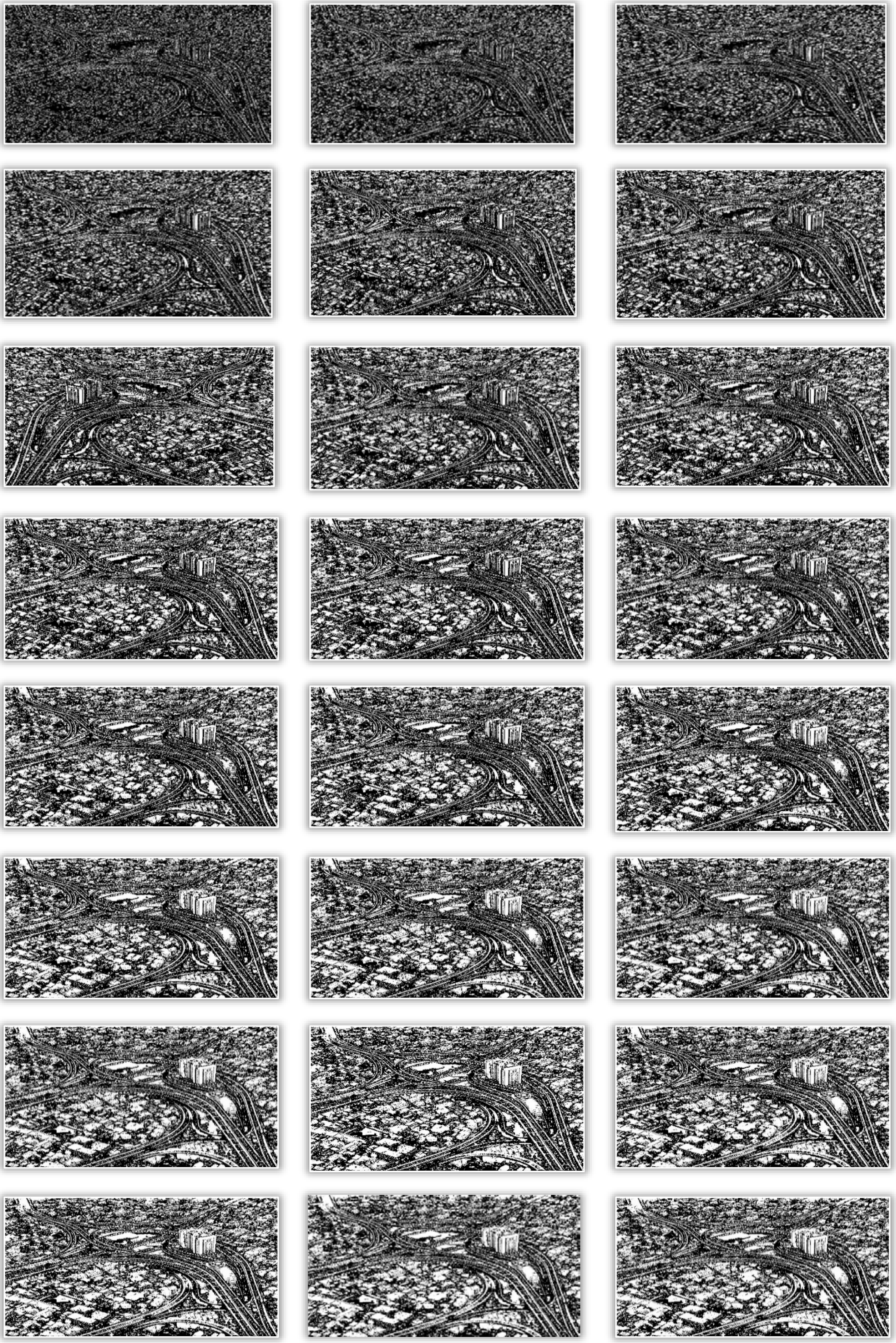

Figure 5. Differential morphological profiles (DMP) of the white top-hat

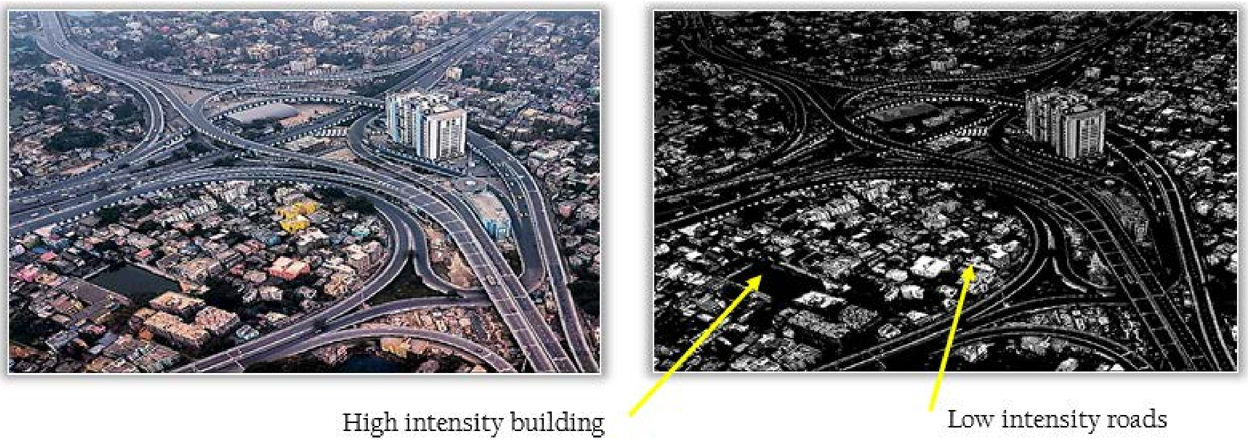

Figure 6. Comparison between final MBI based image and input image

All the buildings with high intensity relative to low intensity roads are extracted. Extracted buildings have intensity greater than MBI value. Few buildings having intensity value more than MBI and situated at far field of the image are being extracted through this process since most of them have low reflectance in the original image. Due to non-zenith location of capturing platform side wall of some of the buildings are highlighted along with high reflectance rooftops. The effect of variation in length of structure element (SE) plays a key role since the structure of buildings to be extracted depends directly on it. For the second condition respective values related to sizes of SE are chosen as $s_{max} = 45, s_{min} = 2$ and $\Delta s = 4$. Comparison between two morphologically processed output images associated with two SE arrays of different lengths are illustrated in Figure. 7. The obtained results clearly indicates that reduction in number of scales have omitted some building structures not fitted in the constructed new SE and that have been clearly indicted with arrow sign.

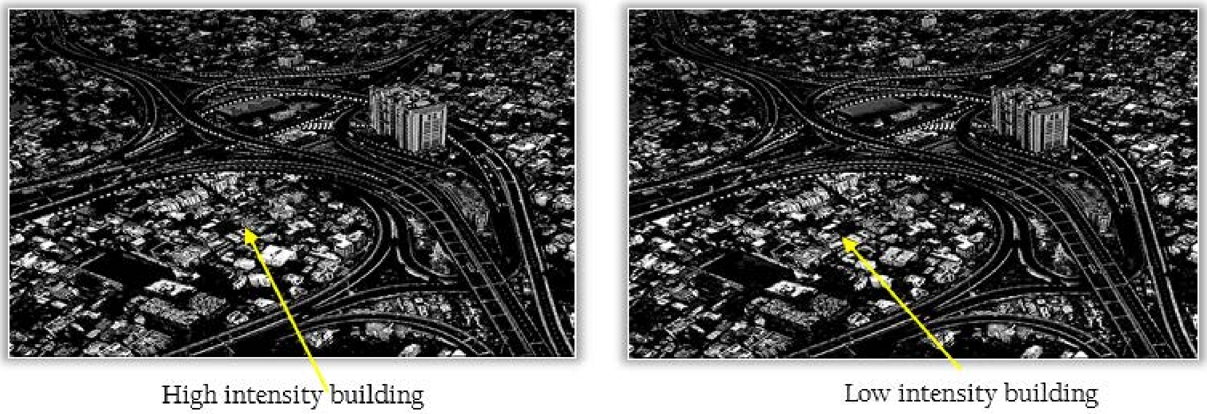

Figure 7. Comparison between two final MBI based images having (a) *S*=25 (b) *S*=12.

— Satellite based image of Chicago, Illinois, US

A satellite-based image of Chicago, Illinois, United States captured in April,2012 [21] has been considered for the second case study. The image as shown in Figure 8 has three visible bands along with 612X612 pixels. The image includes buildings with variable structures, river, low intensity roads, hard soil etc. This image is captured from zenith position resulting in almost uniform reflectance of the buildings with different structured rooftops. The range of pixels intensity lies within 3 to 255 referring low to bright extremum. The values of s_{max}, s_{min} and Δs are chosen as $s_{max} = 50, s_{min} = 2$ and $\Delta s = 2$ for the present study.

Figure 8. Satellite based image of Chicago, Illinois, United States

The number of scales is found to be *S*=25. In Figure 9 some of the eroded images (total 25 erosion images) that have been obtained using morphological opening operation are shown. This erosion of the input image is obtained using element in SE in succession. Morphological reconstruction is performed using *imreconstruct* function by passing two images as marker and mask. In reconstructed output image, all the intensity fluctuations except the intensity peak have been removed which is illustrated in Figure. 10.

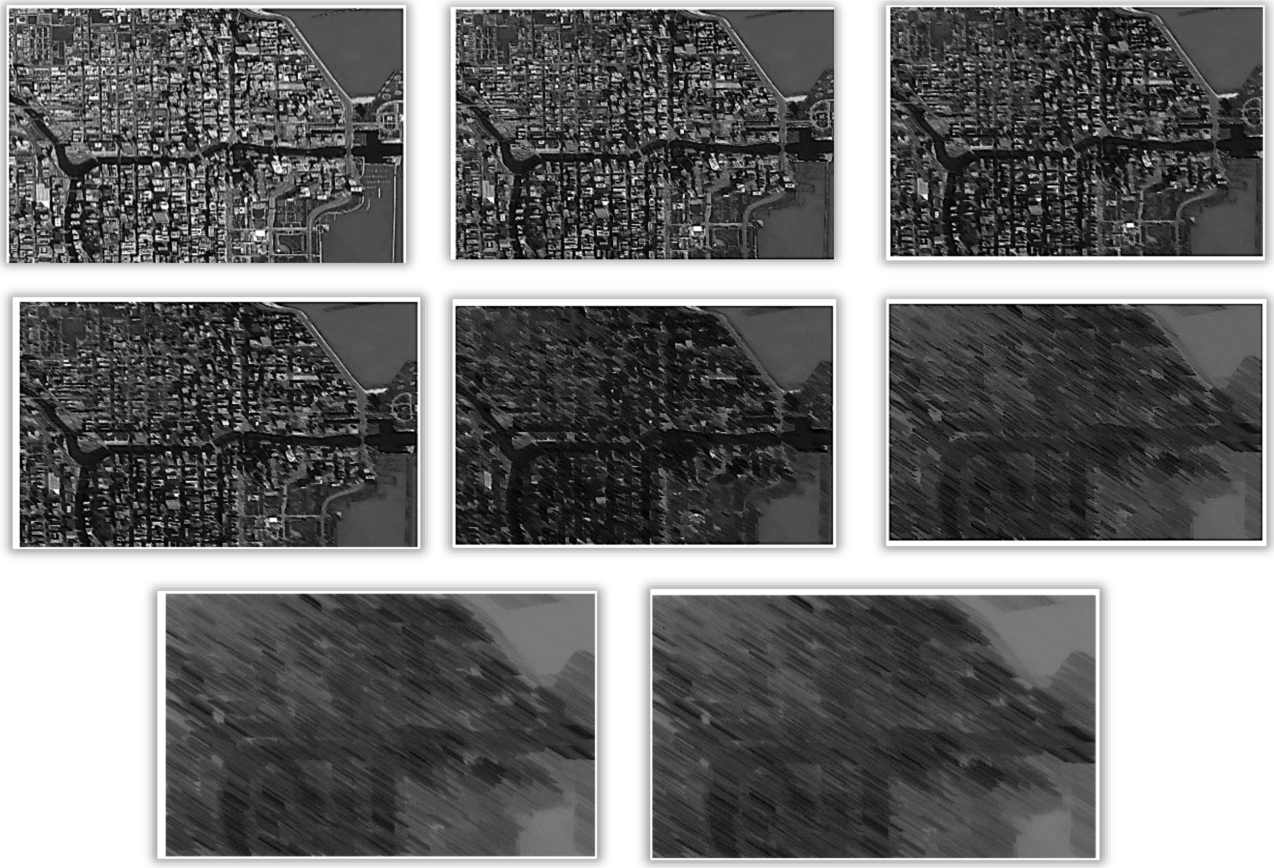

Figure 9. Eroded images obtained using morphological opening operation

Figure 10. Morphologically reconstructed image

Differential morphological profiles (DMP) of the white top-hat have been obtained over the length of linear SE with Δs interval between the profiles to highlight contrast between high reflective rooftops and the shadows adjacent to the buildings. Figure. 11 illustrates all the 25 nos. of DPM (S=25) for each element in linear SE.

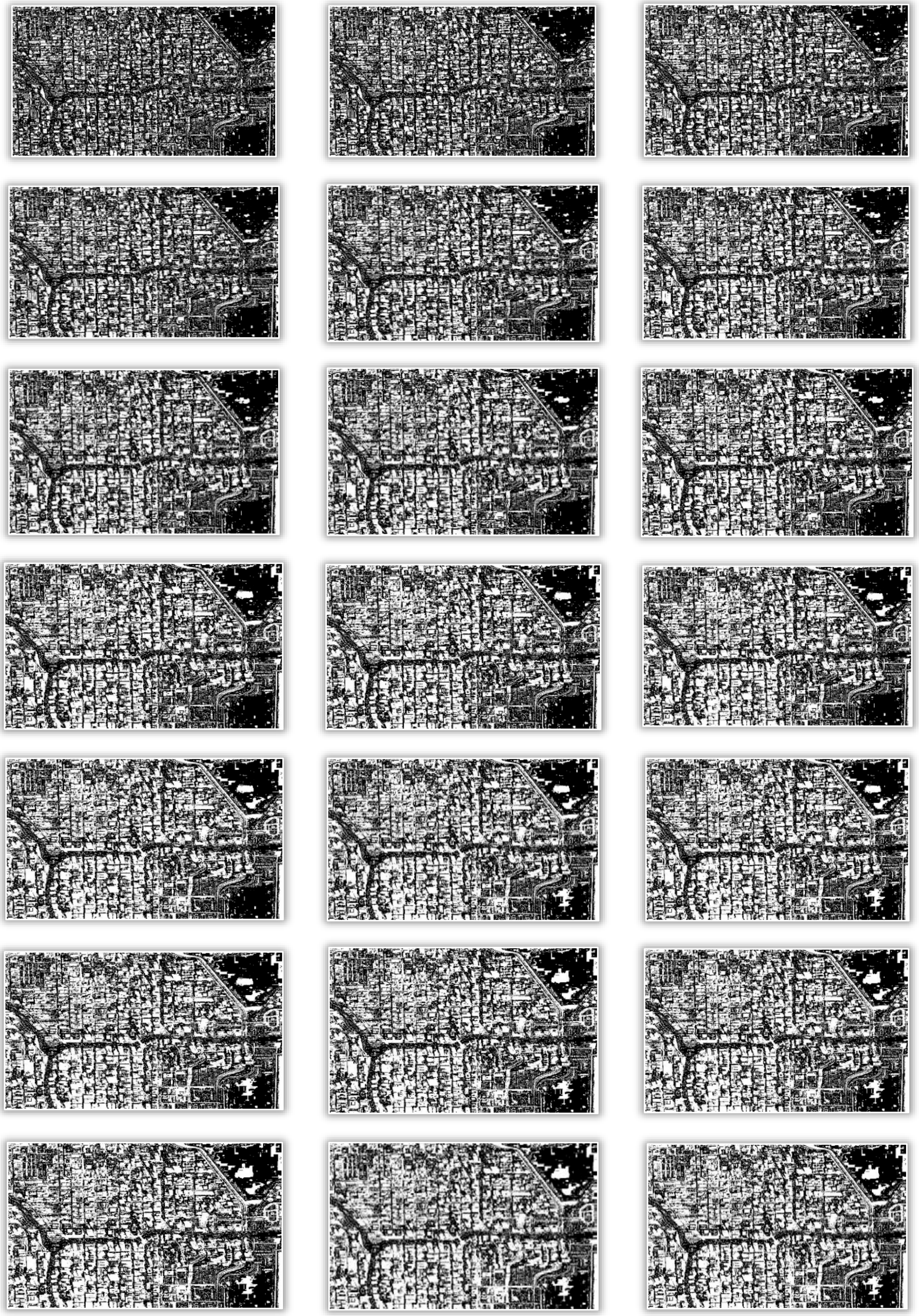

Figure 11. Differential morphological profiles (DMP) of the white top-hat

Depending on the obtained MBI value based on directionality and scale of the profile, intensity adjustment in the final image has been performed to increase the difference between low and high intensities regions. In Figure. 12 the final output image indicating extracted buildings is compared with the input image.

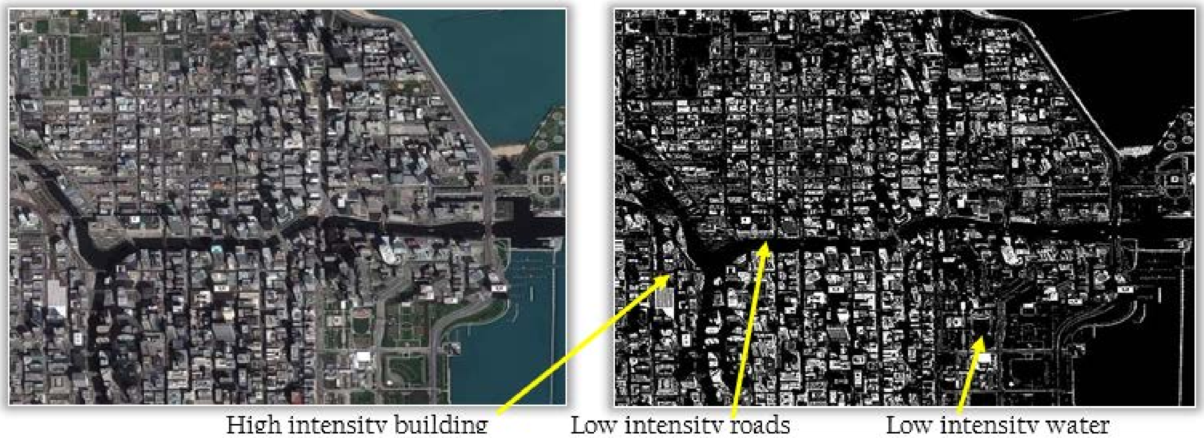

Figure 12. Comparison between final MBI based image and input image.

All the buildings with higher values of MBI have been extracted relative to low intensity roads and water. In this case most of the buildings are extracted since all of them have equal intensities in original image. High reflectance rooftops of all the buildings have been filtered since capturing platform i.e., satellite in this case is in zenith position. Moreover, normalized difference vegetation index (NDVI) has not been considered since the image under study contains less vegetation. It is applicable for the first case study also. In addition, total elapsed time during the execution for the first case study is 15.7158 seconds and that of the second case study is 22.8519 seconds, which indicates the fast processing of this automated method. Since applications of solar panel is increasing by leaps and bounds and installation areas like building roof tops are more preferrable, these automated buildings can further be processed for identification of building roof tops.

4. CONCLUSIONS

In the present communication an automated method for building extraction based on Morphological Building Index (MBI) and Differential morphological profile (DMP) has been elaborated along with different aspects e.g., variation of length of linear SE and the position of image capturing platforms. Length of SE is very important as shape and sizes of the buildings to be extracted depends on it directly which have been reflected from the above two case studies. Two types of remotely sensed images have been considered i.e., satellite and droned based having zenith and non-zenith positions of the capturing platforms. Effects of position of capturing platform has been analysed since the buildings illustrates different position based reflectance. This method of automatic building extraction requires less human intervention and processing time. However, images with less vegetation have been taken for the present experiment that leads to non-implementation of normalized difference vegetation index (NDVI) and also pave the way for future scope of work.

References

[1] Mayer, H: Automatic object extraction from aerial imagery: A survey focusing on buildings. Computer Vision and Image Understanding,74(2):138–149, 1999.
[2] Krishnamachari, S. and Chellappa, R: Delineating buildings by grouping lines with mrfs. IEEE Trans. Image Processing, 5(1):164–168, 1996.
[3] Irvin, R. and McKeown, D: Methods for exploiting the relationship between buildings and their shadows in aerial imagery. Proc. SPIE, 19(6):1564–1575, 1989.
[4] Davis, L: Hierarchical generalized hough transforms and line-segment based generalized hough transforms. IEEE Trans. on Pattern Recognition, 15(4):277–285, 1982.
[5] Lavigne, D; Saeedi, P; Goldstein, N and Zwick, H: Automatic building detection and 3d shape recovery from single monocular electro-optic imagery. SPIE Defense and Security Symposium, 6567, June 2007.
[6] Fraser, C; Baltsavias, E and Gruen, A: Processing of ikonos imagery for submetre 3d positioning and building extraction. ISPRS Journal of Photogrammetry and Remote Sensing, 56(3):177–194, April 2002.
[7] Scholze, S; Moons, T and Van Gool, L: A probabilistic approach to building roof reconstruction using semantic labelling. In Proceedings of the 24th DAGM Symposium on Pattern Recognition, page 257 ff., 2002.
[8] Weidner, U and Forstner, W: Towards automatic building extraction from high-resolution digital elevation models. ISPRS Journal of Photogrammetry and Remote Sensing, 50(4):38–49, August 1995.
[9] Fischer, A; Kolbe, H, T and Lang, F: Integration of 2d and 3d reasoning for building reconstruction using a generic hierarchical model, September 1997.
[10] Cheng, H; Chen, Y and Jiang, X: Thresholding using two-dimensional histogram and fuzzy entropy principle. IEEE Trans. on Image Processing, 9(4):732–735, April 2000.
[11] Peng, J and Liu, C.U: Model and context-driven building extraction in dense urban aerial images. Int. Journal of Remote Sensing, 26:1289– 1307(19), April 2005.
[12] Heuel, S and Kolbe, H. T: Building reconstruction: The dilemma of generic versus specific models. Knstliche Intelligenz, KI, 15(3):57–62, 2001.
[13] Jaynes, C; Riseman, E and Hanson, A: Recognition and reconstruction of buildings from multiple aerial images. Computer Vision and Image Understanding, 90(1):68–98, April 2003.
[14] Lin, C and Nevatia, R: Building detection and description from a single intensity image. Computer Vision and Image Understanding, 72(2), 101–121, 1998.

[15] Wei, Y; Zhao, Z and Song, J: Urban building extraction from high-resolution satellite panchromatic image using clustering and edge detection. In Geoscience and Remote Sensing Symposium, 2004. IGARSS'04. Proceedings. 2004 IEEE International (Vol. 3, pp. 2008–2010). IEEE.

[16] Jin, X and Davis, C.H: Automated building extraction from high-resolution satellite imagery in urban areas using structural, contextual, and spectral information. EURASIP Journal on Advances in Signal Processing, 2005(14), 1–11.

[17] Huang, X and Zhang, L. A: multidirectional and multiscale morphological index for automatic building extraction from multispectral GeoEye-1 imagery. Photogrammetric Engineering & Remote Sensing, 77(7), 721–732, 2011.

[18] Singh, K.K. and Mehrotra, A: Building extraction from VHR imagery using morphological shadow and building operator. In Computing for Sustainable Global Development (INDIACom), 2014 International Conference on (pp. 463–467). IEEE.

[19] Sohn, G and Dowman, I: Extraction of buildings from high-resolution satellite data. In Proceedings of the First Annual Conference of the Advanced School for Computing and Imaging, pages 345–355, 2001.

[20] Huang, X and Zhang, L: Morphological Building/Shadow Index for Building Extraction From High-Resolution Imagery Over Urban Areas, in IEEE Journal of Selected Topics in Applied Earth Observations and Remote Sensing, vol. 5, no. 1, pp. 161-172, Feb. 2012.

[21] Satellite Image of Chicago, Illinois, United States, Collected on April, 2012. Digital photograph, Accessed 9th Aug, 2021, (Creator: DigitalGlobe via Getty Images).

ISSN 1584 – 2665 (printed version); ISSN 2601 – 2332 (online); ISSN-L 1584 – 2665